Open Archive Toulouse Archive Ouverte (OATAO)

OATAO is an open access repository that collects the work of Toulouse researchers and makes it freely available over the web where possible

This is an author's version published in: http://oatao.univ-toulouse.fr/27610

Official URL: https://doi.org/10.1016/j.surfcoat.2020.125521

Any correspondence concerning this service should be sent to the repository administrator: tech-oatao@listes-diff.inp-toulouse.fr

Integrated self-healing coating system for outstanding corrosion protection of AA2024

Yolanda Castro[a,*], Eren Özmen[a,b], Alicia Durán[a]

[a] Instituto de Cerámica y Vidrio (CSIC), Kelsen 5, 28049 Madrid, Spain
[b] CIRIMAT, Université de Toulouse, CNRS, INPT, UPS, 31030 Toulouse, France

A R T I C L E   I N F O

A B S T R A C T

This work reports the preparation of an integrated self-healing system that combines the anodization of Al-substrates with the deposition of environmentally friendly coatings prepared by sol-gel for obtaining an active corrosion protection of aluminum alloys AA2024. The system consists on a first step of forming appropriate anodized layers by controlling the potential and anodizing time. The second step is the infiltration of a cerium sol-gel sol and deposition of a Ce-glass like film, followed by a final hybrid silica sol-gel coating, creating an adherent, stable and active corrosion protective system. SEM, electrochemical techniques (potentiodynamic and EIS tests) as well as an accelerated corrosion test are used to analyze the structure of the coatings and to study the corrosion behavior of the different coatings on AA2024. The results of potentiodynamic measurements showed the excellent corrosion properties and EIS measurements confirmed the self-healing behavior by blocking the pitting defects. The outstanding self-healing corrosion protecting behavior provided by this integrated self-healing coating system offers an efficient chromium-free system for substituting chromium CCC and CCA coatings.

1. Introduction

Aluminum and aluminum alloys are used in many industrial applications due to their promising properties such as strength, lightness, recyclability and formability [1]. Numerous aluminum alloys are already in use for different applications in structural automotive, aviation and aerospace industries. Specifically, the aluminum alloy AA2024 is extensively used due to its suitable properties under mechanical stresses such as bending, multi directional forces, tensile and compressive stresses. However, the application of aluminum alloys is restricted by their high chemical activity and potentially poor corrosion resistance under extreme environment conditions. The inhomogeneous distribution of copper in the alloy microstructure is a major cause of low resistance to pitting and stress corrosion. A rapid physical change in stress level on a specific area of the metal can also causes both chemical and physical variations, thus, making the surface more sensitive to accelerated corrosion.

There are several methods employed in industry for preventing corrosion such as chemical treatments and deposition of coatings; the most efficient systems are chromate conversion coatings (CCC). They are applied on metal surfaces by spraying or immersing the metal into aqueous solutions of chromic acid and chromium salts. The chromate conversion coating contains primarily Cr^{6+}, which acts repairing and locking imperfections and defects in the coating, with the well known "*self healing*" effect. Chromate coatings also provide an excellent porous surface favoring the adhesion with many different primers and top coats [2 5]. However, the environmental and human health risk associated with the use of Cr^{6+} ions are the origin of the total ban of its use in Europe from 2007 in every industrial sectors excepting aeronautic and aerospace sectors [6].

A lot of work has been developed from the beginning of 2000 decade for solving this problem, searching alternatives for replacing chromate coatings. One main route has been the use of hybrid silica organic inorganic coatings prepared by sol gel and densified at low temperature [7,8]. These coatings combine the properties of organic components (flexibility, high density, and compatibility with paint systems) with those of inorganic components (scratch resistance, durability, etc.). Different authors have reported the preparation of silica sol gel films on AA2024 aluminum alloys using 3 glycidoxypropyl trimethoxysilane (GPTMS), mercaptopropyltrimethoxysilane (MPTS) or methyltriethoxysilane (MTES) as hybrid organic inorganic precursors, and tetraethoxysilane (TEOS) as inorganic source, showing efficient corrosion protection on AA2024 alloy [9 11]. In general, the control of the synthesis parameters and the incorporation of different organic

monomers and inorganic nanoparticles allow obtaining coatings with tailored and suitable properties such as density, hydrophilicity/hydro phobicity and good physical barrier.

However, even though silica sol gel coatings successfully act as physical corrosion barriers, they do not provide self healing effect only delaying the corrosion development. The addition of environmentally friendly inhibitors such as cerium to the hybrid coatings is a good strategy to generate an active protection [12,13]. Electrochemical characterization of silica sol gel coatings on aluminum alloys prepared with and without cerium inhibitor usually show that the inhibited systems present better corrosion properties than those non inhibited and provide a self healing protection [14]. Encapsulation of inhibitors in nano containers is other proposed solution [15]. Many different nano containers have been tested. For example, Zheludkevich et al. reported the preparation of SiO_2 particles coated with poly(ethylene imine)/poly(styrene sulfonate) (PEI/PSS) polyelectrolyte layers, the organic inhibitor (benzotriazole) being entrapped within the polyelec trolyte multilayers. Then, the nano containers are incorporated into organosiloxane sols and deposited on AA2024 substrates. Electro chemical impedance results reveal that coatings without nano con tainers showed corrosion immediately after immersion in 0.05 M NaCl. When nano containers are added corrosion slightly decreases after 40 h of immersion [16 18]. Indeed, abundant results show that the im provement in the corrosion behavior of Al alloys is not enough to substitute successfully CCC and CAA coatings. The most important limitation relates with the maximum concentration of inhibitor that can be introduced in the coatings. Concentrations higher than 5% mol for inorganic and ~1% mol for organic inhibitors lead to the formation of defects, generating porous structures that reduce the barrier properties and deactivate the inhibiting properties of the coatings [19 21].

Other approach was the use of Ce based sol gel sols for producing Ce glass like coatings that provide self healing effect [22,23]. Efficient self healing behavior was proved by EIS and electrochemical techni ques, and standard industrial tests (SST ISO 9227, immersion emersion test DIN EN 3212, Filiform corrosion test, EN ISO 3665, Adhesion on embossing, ISO 6272 2 2002, Cracking on T bend, ECCA T7 1996) [24] confirmed the good performance of these coatings. However, their ef ficiency is not enough for aircraft industry.

On the other hand, the use of anodization process using environ mental electrolytes to protect the aluminum against corrosion is gaining more and more attention. Anodizing is a process where the thickness of natural aluminum oxide layer increase through an electrochemical re action using acidic electrolytes [25 29]. The acidic electrolyte solution slowly dissolves the aluminum oxide layer while the oxidation takes places with the formation of a new layer with nano pores with a dia meter between 10 and 100 nm. After anodizing of aluminum, surface becomes generally stronger, harder and more adherent than before treatment [30,31]. M. Xiangfeng et al. created a protective aluminum oxide layer on A2024 aluminum alloy by using sulfuric and citric acid for anodizing. The anodized layer was tested in a 3.5 wt% NaCl aqueous solution and a corrosion potential of -0.7 V was observed compared to -0.58 V of bare substrate [32], showing that the anodized film was acting as an efficient corrosion barrier. However, anodization process is not enough to create a full protection system against corrosion; more over, in some cases this layer reduces the paint adhesion.

Thereby, great efforts are underway to identify efficient alternative systems with desirable surface properties combining anodizing with other protecting coatings [33,34]. M. Whelan et al. reported the pre paration of nano porous oxide films on AA2024 T3 aluminum alloys by anodizing with further loading of pores with organic inhibitors by im mersion in aqueous solutions of 1H benzotriazole (1,2,3), imidazole (DPTZ) or 3,6 Di 2 pyridyl1,2,4,5 tetrazine (DPTZ). The systems are sealed by maintaining the samples for 2 weeks at room temperature permitting to grow a natural hydration coating; other route used is the hydrothermal sealing in boiling deionized water. Neutral salt spray (5 wt% aqueous NaCl solution) and electrochemical impedance

Table 1
Sample identification.

Labelled	Samples
Al-2024	Bare AA2024 substrate
A1	Bare AA2024 substrate + anodized coating, 12 V-10 min
A2	Bare AA2024 substrate + anodized coating, 12 V-20 min
A3	Bare AA2024 substrate + anodized coating, 12 V-30 min
A3-GTL	Bare AA2024 substrate + anodized coating + hybrid silica coating
A3-GTL2	Bare AA2024 substrate + anodized coating + two hybrid silica coating
A3-Ce-GTL	Bare AA2024 substrate + anodized coating + cerium glass-like coating + hybrid silica coating

spectroscopy (3.5% w/v NaCl) showed that 3,6 Di 2 pyridyl 1,2,4,5 tetrazine inhibitor has a positive effect in the barrier properties and pit suppression on the anodized AA2024 alloys. The nitrogen compounds improve the sealing of the anodized coating. However, the EIS low frequency results, Log/Z/, show a rapid degradation of coating re sistance, decreasing from 108 Ohms in the initial stage down to 105 in 168 h. The same authors studied the corrosion behavior of silica and silica/zirconia sol gel coatings deposited on anodized aluminum sur faces by neutral salt spray and electrochemical impedance spectro scopy. The penetration of the sols in the porous anodic film was clearly observed by EDX but the corrosion behavior depends on the anodizing process and on the synthesis route of sol gel sols. Impedance values increase for the system that combines anodization with deposition of phenyl functionalized silica sol, compared to only anodized samples. These systems improve the barrier properties of anodized AA2024 substrates but no self healing behavior is detected. Moreover, when organic inhibitors are introduced in these systems a rapid degradation of log/Z/ is observed [35 37]. M. Terada et al. [38] reported the pre paration of samples combining the anodization process with a hydro thermal treatment using Ce (III) aqueous solutions, with a further de position of a silica sol gel coating heat treated at 150 °C for 1 h. EIS results showed that the hydrothermally treated samples improved the corrosion resistance of the AA 2024 T3. However, the curing tem perature used (>120 °C) may affect the integrity of the alloy. More over, some pores and defects appear in the sol gel coating probably associated with the interaction of cerium conversion and sol gel coat ings.

Despite the high number of published articles, there is still no in dustrially suitable solution able to provide the required corrosion pro tection for aircraft aluminum alloys.

The aim of this work was to develop an integrated self healing coating system able to replace the CCC and CAA coatings on aluminum alloy AA2024 by combining the anodizing process with the further deposition of inhibiting and barrier coatings prepared by sol gel. The first step consisted on establishing the suitable anodization conditions, including electrolyte, potential and anodizing time. The intermediate step was the infiltration of the porous structure of anodized layer with a Ce based sol that should act as a reservoir of corrosion inhibitors. A sol gel hybrid silica coating acting as corrosion barrier is the final step. The corrosion behavior of the integrated system was evaluated by electro chemical techniques (potentiodynamic curves and EIS tests), along with an immersion accelerated corrosion test, all revealing an outstanding corrosion behavior with long lasting self healing effect. This integrated approach (anodization process plus inhibitor infiltration plus sol gel barrier coating) constitutes a new route for obtaining active protecting coating systems on AA2024 substrates, opening promising perspectives to replace CCC or CAA coatings.
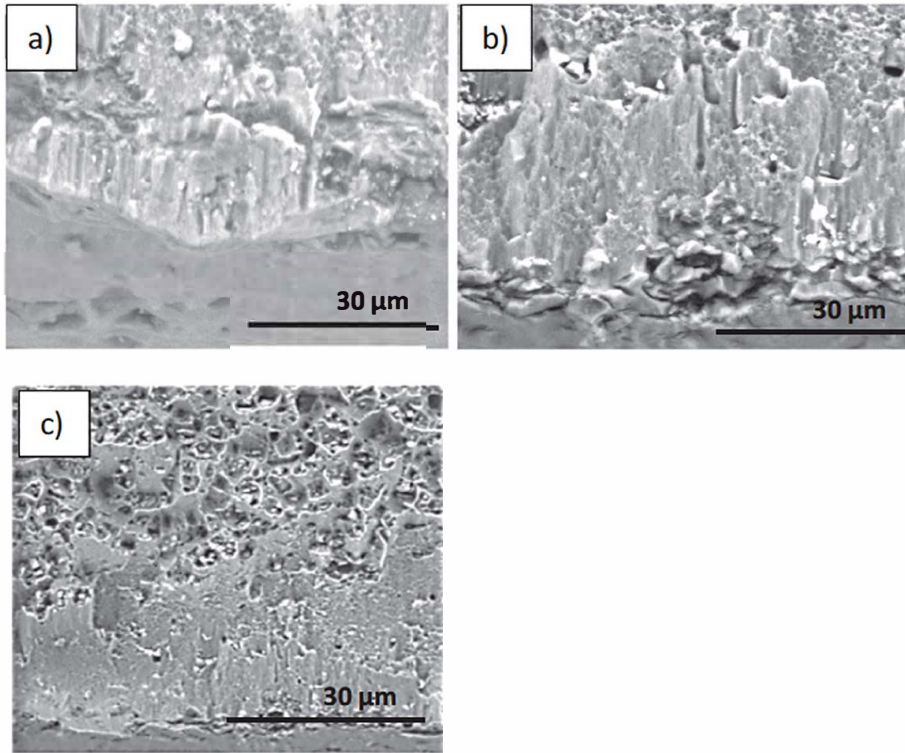
Fig. 1. SEM images of cross-sectional substrate of anodized using H_2SO_4 at 12 V during a) 10 min, b) 20 min and c) 30 min.

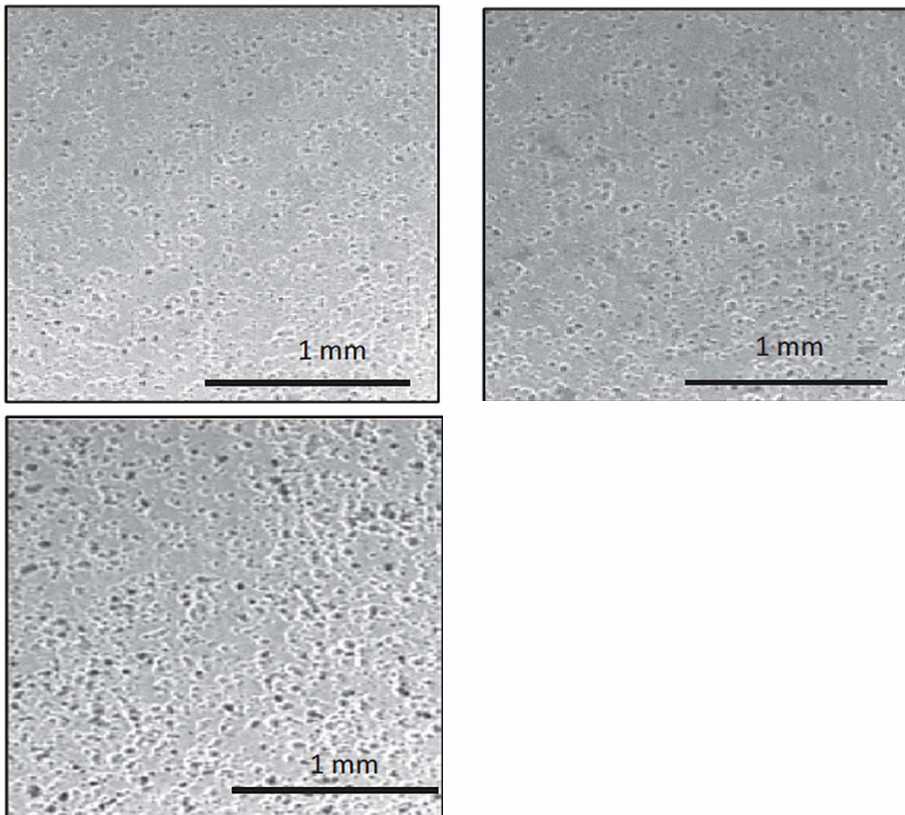**Fig. 2.** SEM images of surface of anodized substrate using H_2SO_4 at 12 V during a) 10 min, b) 20 min and c) 30 min.
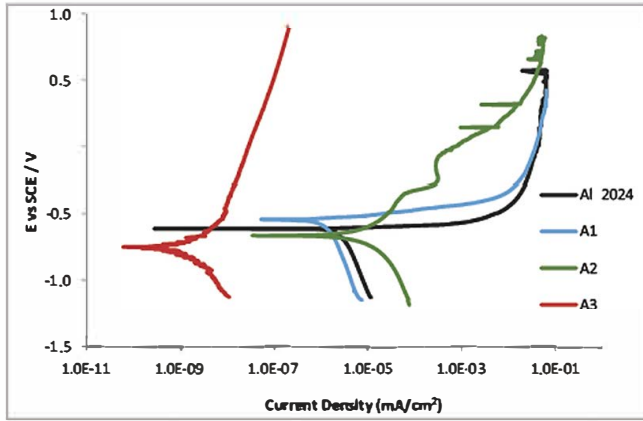
Fig. 3. Potentiodynamic curves of bare A2024 substrate and anodized samples at different anodizing time.

Table 2

Corrosion potential (E_{corr}) and passive current density of anodized AA2024 at 12 V at different times, anodized surface coated with one or two silica sol-gel coatings and integrated hybrid silica self-healing coating.

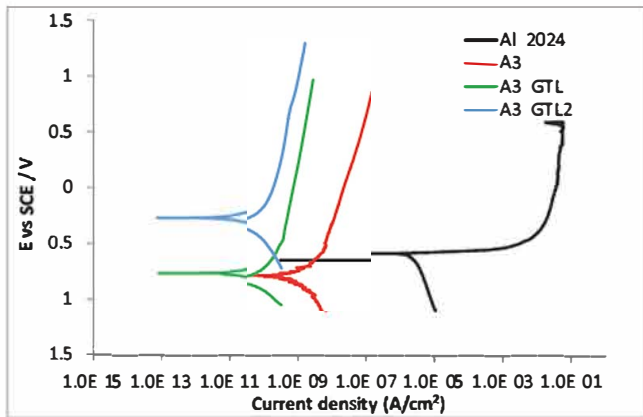| Samples	E_{corr} [V vs SCE]	Passive current density (A/cm²)
Al-2024	0.58	–
A1	0.57	–
A2	0.58	–
A3	0.73	~4.0E 8
A3-GTL	0.75	~7.1E 10
A3-GTL2	0.32	~3.9E 10
A3-Ce-GTL	–	≤1.0E 12

Fig. 4. Potentiodynamic curves of bare A2024 substrate, anodized sample and anodized surface coated with one (A3-GTL) and two (A3-GTL2) silica sol-gel coatings.

2. Experimental procedure

2.1. Substrate cleaning and anodization process

AA2024 T3 substrates with dimensions $2 \times 4 \times 0.2$ cm³ and composition (wt%) of 4.67% Cu, 0.05% Si, 0.21% Fe, 1.5% Mg, 0.64% Mn, 0.029% and Ti, 0.07% Zn, were pre cleaned using an industrial process including an alkaline cleaned solution (Metaclean T2001 Chemie Vertrieb Hannover GmbH & Co KG), an alkaline etching solution (Turco Liquid Aluminetch Nr.2 Turco Chemie GmbH), and an acid etching solution (Turco Liquid Smutgo NC Turco Chemie GmbH).

The anodizing process developed on pre cleaned samples using a power supplier (Labconco 1000 Volt, Kansas City US). A graphite plate was used as anode and pre cleaned AA2024 aluminum alloy as cathode.

Two acid solutions were tested: 2.5 M sulfuric acid H_2SO_4 (VWR, 96.5%) and 1 M phosphoric acid H_3PO_4 (Pancreac, 85%). The anodization process was performed by applying a constant voltage of 12 V for 10 to 30 min, always under stirring.

2.2. Synthesis of hybrid silica and cerium sols

A silica sol, denoted as GTL, was prepared by mixing 3 (glycidyloxypropyl)trimethoxysilane (GPTMS, (ABCR, 98%)), TEOS (Aldrich, 99%) and colloidal silica suspension (LUDOX (40 wt%)). Then, nitric acid (NHO₃ (VWR, 65%)) was added under vigorous stirring up to complete the chemical reactions. As final step, ethanol (EtOH (Pancreac, 99.8%)) is added to obtain a SiO_2 concentration of 180 g/L.

An inorganic cerium sol (Ce sol) was also prepared following the process described in [23,24]. First, Cerium(III) nitrate hexahydrate (Ce (NO₃)₃6H₂O (Aldrich, 98%)) and EtOH (Pancreac, 99.8) were mixed following with the addition of acetic acid (AcH (Merck, 100%)), citric acid (VWR, 99.8%), and butanediol (Aldrich 99%).

The wettability of both sols was measured by using the 'Easy Drop Standard' analysis system (Kruss DSA 100) equipment. A volume of 0.8 1 μL of sol was dropped on surface of A2024 substrate and the contact angle was measured by recording a video after every dispensed sol droplet. The measurements were performed for each sol (GTL and Ce sols) and the results are presented as average ± SD.

The stability of the sols was evaluated using an A&D Vibro Viscosimeter SV 10 to follow the variation of the viscosity as a function of time.

2.3. Deposition of coatings and thermal curing

The deposition process was carried out with a dip coater to obtain single and multiple silica layers. Ce sol was infiltrated in the porous anodized layer by dip coating depositing a Ce coating at 25 cm/min. GTL sols were deposited on bare and anodized substrates as well as on previously Ce infiltrated anodized substrates, at room temperature at a withdrawal rate of 25 cm/min. Table 1 summarizes the different coating systems prepared. The coatings were sintered at 120 °C for 1 h. For double GTL2 coatings, an intermediary step was applied using a hot air gun at 80 °C/1 min followed by sintering at 120 °C.

The thickness was measured on coated glass slides by Spectroscopic Ellipsometer (J.A. Woollam Co., Inc., EC 400, M 2000U Software: WVASE32). The spectral band was recorded from 250 nm to 900 nm at incident angles between 50° and 60° fitting the data with WVASE32 software with a Cauchy model. Table 1 presents the description and labelling of all the studied systems.

2.4. Characterization of the protective coating systems

The surface morphology of the anodized layers was analyzed by scanning electron microscopy (SEM (HITACHI TM 1000)). The anodized substrates were prepared bending the samples over 180° to generate micro cracks in the alumina layer [35].

Adhesion test was carried out using a Cross Hatch Adhesion Tester, (NEUTREK Instruments Company), following the ASTM D3359 standard. The test was performed with a multi blade cutting tool to make a lattice pattern with several cuts in each direction on the coating. Then, a line of tape was applied over the pattern and removed. Before and after test, the pattern was observed by optical microscopy (Axiophot ZEISS, software; ZEN 2012). The visual evaluation allows the classification of the defects from 0 to 5A, where the higher number represents less peeling.

The corrosion resistance of bare AA2024 substrate, anodized samples and integrated hybrid coatings were evaluated by potentiodynamic tests in 3.5 wt% NaCl (aq) at room temperature using a Gamry FAS2 Femtostat equipment. A typical three electrode cell was used; a saturated calomel electrode (SCE) as reference electrode, a platinum wire as
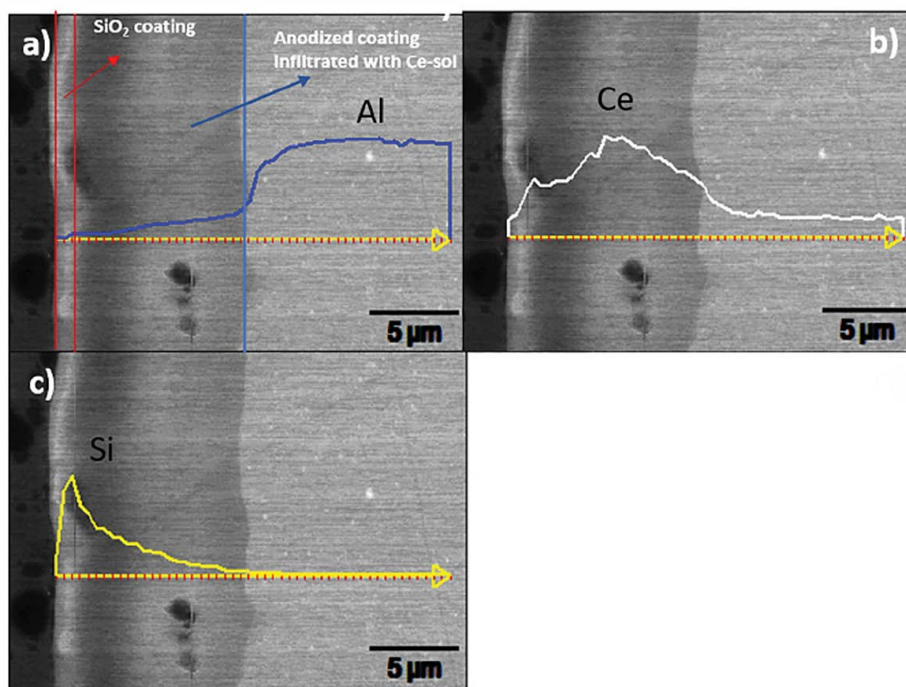
Fig. 5. Transverse section of A3-Ce-GTL system observed by SEM-EDX analysis of Al a), Ce b) and Si c) in line-scan mode.
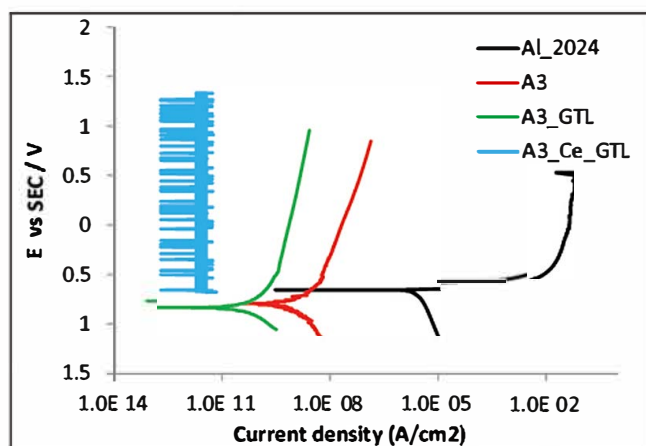

Fig. 6. Potentiodynamic curves of bare AA2024, A3, A3-GTL and integrated coating system A3-Ce-GTL.

counter electrode and the tested samples as working electrode (exposed area 0.65 cm^2). Before each measurement, the samples were immersed in the electrolyte for 1 h and the open circuit potential (E_{oc}) was registered up to reach the equilibrium. The corrosion potential (E_{corr}) and the corrosion current density (j_{corr}) were determined using the software Gamry My Data.

To observe the chemical composition of integrated coating system (A3 Ce GTL coating), Field Emission Scanning Electron Microscopes (FE SEM, Hitachi S 4700) coupled with X ray energy dispersive unit was used.

Electrochemical impedance spectroscopy (EIS) tests were also performed using a Gamry FAS2 Femtostat equipment and applying an AC voltage at the open circuit potential with sinusoidal amplitude of 10 mV, from a frequency of 106 Hz down to 10^{-1} Hz. The electrolyte used was a 3.5 wt% NaCl (aq) and the area exposed 0.65 cm^2. A defect was introduced by hammering a thin needle (insulin syringe) of 300 μm in diameter. After EIS measurement, FE SEM (Hitachi S 4700) was used to analysis the defect.

Finally, an accelerated corrosion test was performed by immersing the samples in 3.5 wt% NaCl (aq) solution at room temperature to follow the evolution of corrosion process. Samples were placed in flasks and covered with a volume of 120 mL of NaCl solution. The area of sample exposed to electrolyte was 6.2 cm^2, according to the standard guide for laboratory immersion corrosion testing of metals (NACE/ASTM TMO169/G31). Immersed samples were visually evaluated as a function of immersion time from 1 to 75 days.

3. Results and discussion

3.1. Characterization of the sols and coatings

The GTL sols showed a high stability, measured from the evolution of viscosity with time. The viscosity maintained constant for at least 3 weeks for GTL sol and 90 days for Ce sol.

Contact angle was measured to assess the wettability of the sols on pre cleaned AA2024 substrates. A volume of 0.8 1 μL of GTL and Ce sols were dropped on the treated A2024 substrate obtaining contact angles of 27° and 32 36°, respectively. This low values demonstrate that both sols are suitable for obtaining homogeneous coatings after the dipping process (Fig. 1 in the supporting information).

The thickness of GTL single coatings was around 3 μm and the Ce films obtained after infiltration and deposition by dip coating were around 600 nm. For double GTL coatings thickness was 5.3 μm.

Adhesion tests on A3 GTL and A3 Ce GTL samples showed an excellent performance without delamination of scaling in any of the tested samples (Fig. 2 in the supporting information).

3.2. Anodizing process

The anodizing process was studied with two acid electrolytes: 2.5 M sulfuric acid H_2SO_4 and 1 M phosphoric acid H_3PO_4. The potential and current density were monitored during the whole process. For both electrolytes, the voltage was stabilized after 20 s. The current density decreased slightly during the steady state with a further progressive increase, associated with the generation of a passive aluminum oxide layer on the AA2024 surface. Scanning electron microscopy was used to analyze the morphology of all anodized layers.
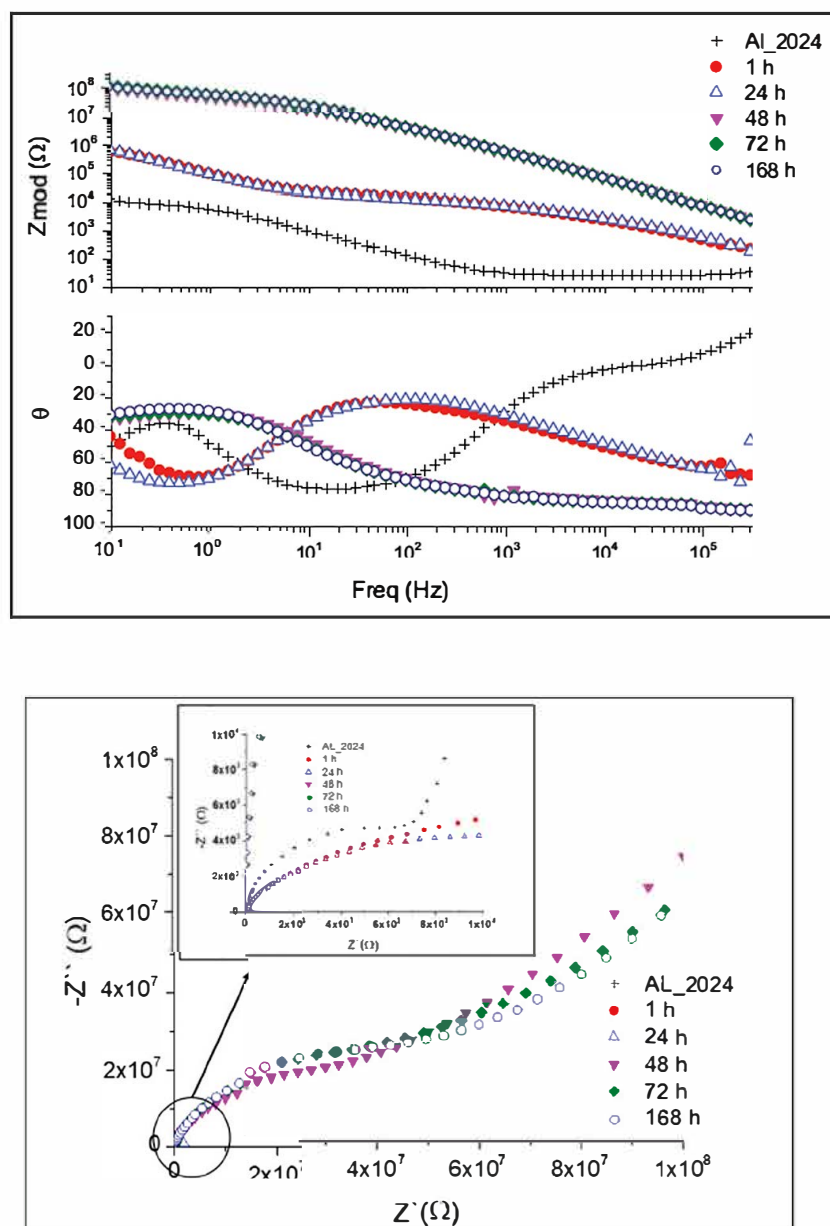
Fig. 7. EIS spectra of bare AA2024 substrate and A3-Ce-GTL integrated system as a function of immersion time in 3.5% NaCl.

Fig. 1 shows the SEM images of cross sectional view of the anodized layers obtained using H_2SO_4 as electrolyte and applying a voltage of 12 V as a function of time. The thickness of anodizing increases with increasing anodization times from 10 to 30 min, reaching a maximum value of ~50 μm. For H_3PO_4 electrolyte, non homogeneous layers were obtained by varying the potential and time. In the selected conditions of applied voltage (10 30 V) and time (10 30 min), it was not possible to obtain reproducible layers for this electrolyte.

The surface morphology of anodized samples obtained using H_2SO_4 (Fig. 2) reveals a non organized porous structure with a narrow pore size distribution. The density and diameter of pores increase from ± 8 10 μm to 15 18 μm with increasing anodizing time. The stronger cavitation effect for longer anodizing time likely explain the generation of more and bigger pores. The density and size of pores obtained at 12 V are likely suitable to act as Ce reservoir in the integrated system.

In the case of H_3PO_4 electrolyte, (Fig. 3 in supported information), the pores grow irregularly in size with increasing the anodizing po tential and time.

From these results, H_2SO_4 electrolyte and 12 V were selected as

appropriate anodizing conditions for the following tests.

The corrosion behavior of bare and anodized aluminum AA2024 obtained at different times at 12 V was analyzed by potentiodynamic curves (Fig. 3). The corrosion parameters such as corrosion potential (E_{corr}) and passive region are included in Table 2. The bare AA2024 substrate shows a corrosion potential (E_{corr}) of − 0.58 V vs SCE pre senting active corrosion above E_{corr}; the current density increases with the increment of potential. For the anodized aluminum alloys, the corrosion behavior strongly changes compared to bare substrate. The sharply decrease in the j_{coor} of anodized AA2024 12 V 30 min substrate indicates that the anodized layer provides a high protection against diffusion of chloride ions to the substrate [11 13]. The evolution of potentiodynamic curves, Fig. 3, shows that a time close to 30 min is necessary to generate an efficient barrier, with an extended passivation range up to 1 V vs SCE. This behavior could likely correspond with a minimum threshold thickness of the anodized layer, around 50 μm, with adequate density and pore size distribution.

From these results, the anodizing conditions were fixed: 2.5 M H_2SO_4 acid solution as electrolyte, potential of 12 V during 30 min,
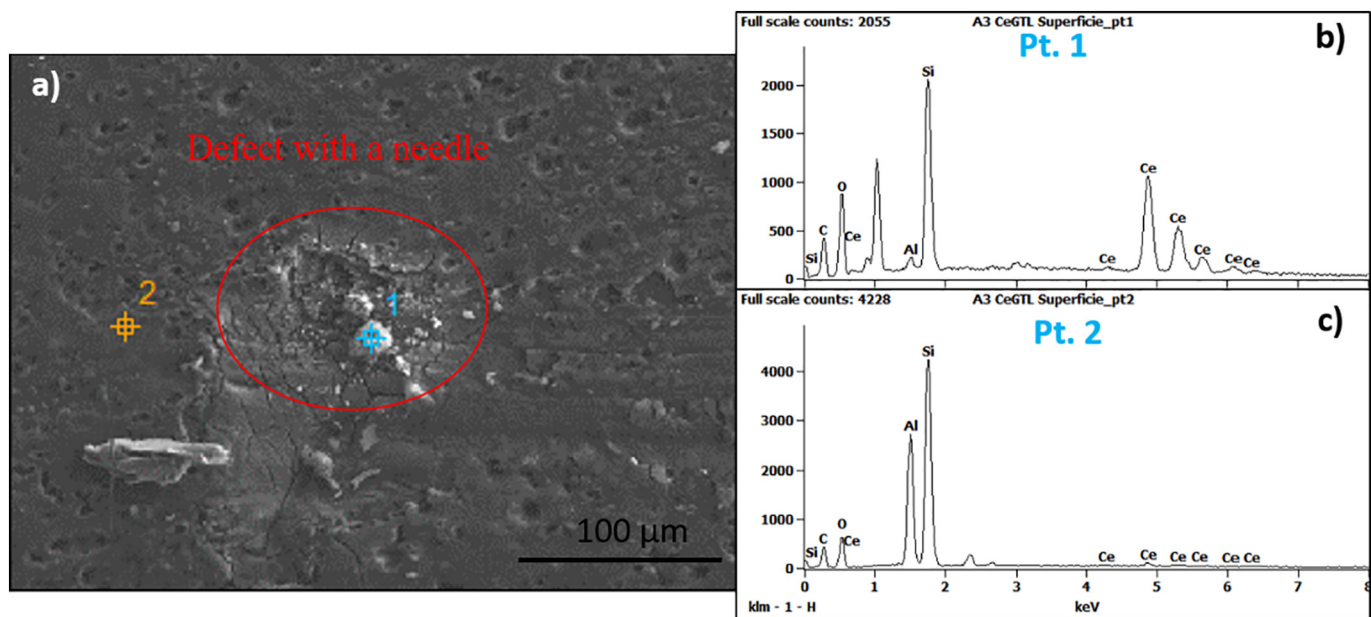
Fig. 8. SEM-EDXS analysis, surface morphology and chemical composition spectra detected on two different areas on A3 Ce GTL coating after immersion for 168 h in 3.5% NaCl.
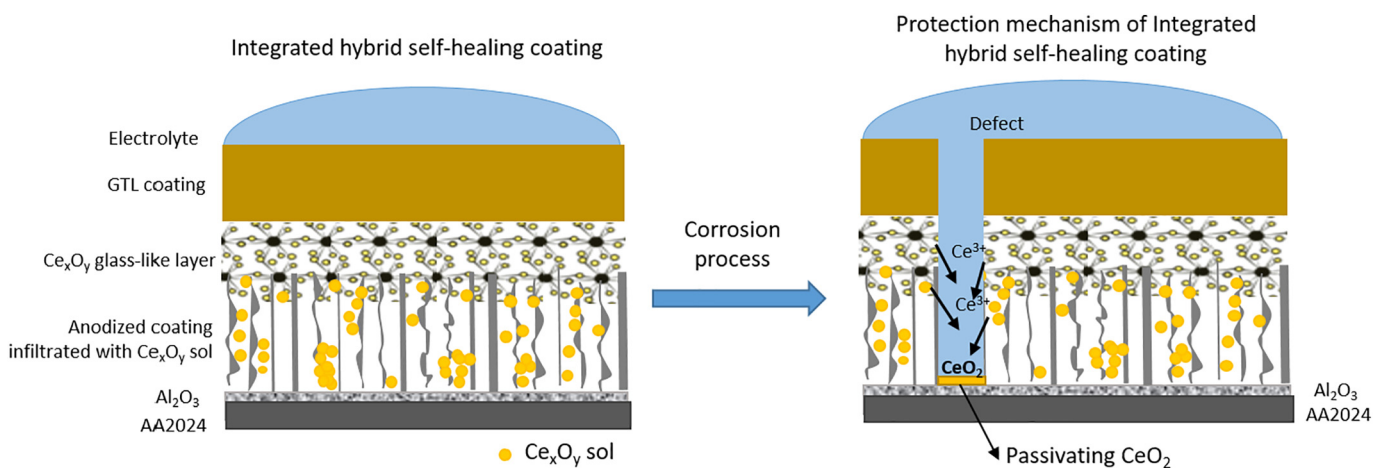

Fig. 9. Schematic illustration of the combined system and protective mechanism of A3-Ce-GTL integrated system.

corresponding to the more protective and homogeneous Al_2O_3 layer with suitable pore size, pore distribution and thickness.

The following step was testing the anodized alloy with a further protection; the deposition of hybrid sol gel GTL coating.

Fig. 4 shows the potentiodynamic curves of AA2024 substrate compared to the A3 anodic layer (12 V/30 min) along with A3 anodized sample coated with one and two hybrid silica coatings (A3 GTL and A3 GTL2, respectively). In all the systems, the anodic and cathodic branches of the polarization curves moved to lower corrosion current density compared to bare AA2024 and A3 sample.

For A3 GTL system, the corrosion potential maintains respecting to A3 sample; however, an E_{corr} shifting to more positive value around -0.32 V vs SCE is observed for A3 GTL2 (Table 2). Furthermore, corrosion current density decreases more than four order of magnitude for A3 GTL and A3 GTL2, respectively compared to AA2024 substrate. A wide passive region appears in the anodic region due to presence of an active barrier effect in all the samples. This passive region is maintained up to potentials higher than 1 V vs SCE. The combination of the anodizing process with the deposition of an organic inorganic sol gel coat (GTL) significantly improves the corrosion protection of aluminum alloys, associated to a very low corrosion current density, higher passive

region and shifting of the E_{corr} to more positive values. The very good adhesion between coatings and substrate benefit this behavior. Indeed, these combined layers show an excellent barrier effect. Although the bi layer shows a slightly better performance, there are not significant differences between the corrosion behaviors of one or two layers of GTL. Thus, for safeguarding an easier transference to an industrial process, that usually require minimizing the number of steps of the total process, the A3 GTL system was selected to further studies.

Although the combined anodized GTL sample shows a very high barrier effect, this system does not include corrosion inhibitors. Therefore, corrosion will develop leading to extended corrosion after the appearance of the first pitting or other defect. The goal is obtaining environmentally friendly systems with high barrier effect also including self healing behavior, able to replace the chromium conversion coatings.

The cerium glass like coating deposited on A3 sample (anodized substrate) by dipping at 25 cm/min using the Ce sol [23,24] focus to provide self healing performance. The infiltration of the anodizing channels with the Ce sol and further deposition of a pure cerium glass like coating should act as a reservoir of corrosion inhibitor. On top of the anodized infiltrated samples a hybrid silica sol gel coating GTL was
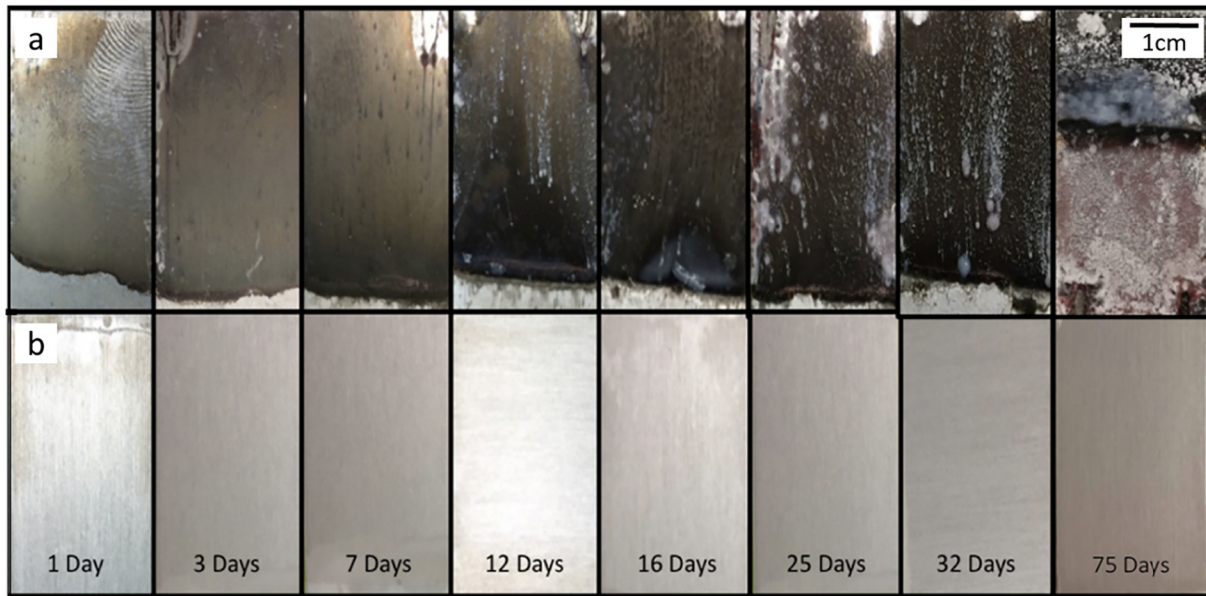
Fig. 10. Images of the corrosion suffered by bare AA20204 substrate a) and integrated self-healing system A3-Ce-GTL b) during 75 days of immersion in sea-water environment.

deposited to create an integrated hybrid self healing coating (A3 Ce GTLsystem). An only GTL coating was applied taking into consideration the good performance showed in Fig. 4. Fig. 5 shows the EDX analysis on a line scan on cross section of A3 Ce GTL coating. EDX analysis was used to plot the profiles of Ce, Si and Al distributions and to confirm the infiltration of the Ce in the anodizing coating. As can be seen, Ce sol filled the pores, and covered the whole surface of anodized coating (Fig. 5c), and no infiltration is detected in the hybrid silica coating (Fig. 5c).

Fig. 6 shows the electrochemical polarization curves of integrated hybrid self healing coating (A3 Ce GTL), compared with A3 GTL, A3 and bare AA2024 substrates tested in 3.5 wt% NaCl solution.

A3 Ce GTL integrated protection system presents an outstanding corrosion behavior; the high resistance does not allow to be measured because the current density is below the detection limit of the equipment (10^{-12} A/cm^2). Up to the best of our knowledge, such high corrosion behavior has not been reported for any of the systems considered to replace CCC and CAA coatings.

Electrochemical impedance spectroscopy confirmed the good anticorrosion behavior and permitted to evaluate the self healing effect of integrated self healing hybrid silica coating.

Fig. 7a shows the bode plots recorded up to 168 h of exposure of the integrated system with a defect of 300 μm introduced with a needle and tested in 3.5% NaCl solution, compared to bare AA2024 substrate. An increment of the impedance modulus at low frequency ($\sim 2 \times 10^6$ Ω) was observed after 1 and 24 h of immersion, this being two orders of magnitude higher than the initial value of bare AA2024 alloy ($\sim 6.4 \times 10^4$ Ω), and confirming the efficient blocking of the system to the electrolyte access towards substrate. More important, after 48 h of immersion, the low frequency value sharply increases up to $\sim 2.8 \times 10^8$ Ω, and this resistance maintained after 168 h of immersion. Considering the initial and big defect introduced in the sample, this increase of the low frequency impedance with the immersion time is likely caused by the migration of cerium ions to the pitting, to precipitate as oxides, hydroxides or even hydrates that passivate and block the big defect introduced. This confirms the self repairing capability of the coating and demonstrates a self healing behavior; similar results not appearing in literature up to our best knowledge. On the other hand, different time constants appear in the Bode phase for immersion times of 1 and 24 h. On the other hand, different time constants appear in the

Bode phase plot for immersion times of 1 and 24 h, with an important shift to lower frequency observed from 48 h, associated with the strong impedance frequency increase described above.

Fig. 8 shows the SEM EDX analysis of the A3 Ce GTL coating after EIS test. A defect performed in the integrated coating system and produced by the insulin needle can be recognized together with the presence of a precipitate. The spectrum on the Point 1 (Fig. 8b) shows the presence of a significant amount of cerium confirming the migration and precipitation of cerium ions to the defect. However, the acquisition on the Point 2 (Fig. 8c) shows the presence of silica and aluminum, associated with the hybrid silica sol gel coating GTL deposited on top of the anodized infiltrated sample and with the substrate, respectively.

Fig. 9 shows a schematic illustration of the A3 Ce GTL integrated system and its corrosion protection mechanism provided. After a pitting of the barrier coating (GTL), the cerium ions are able to migrate from Ce_xO_y coating and/or from the infiltrated channels of anodized coating, passivating the corrosion points of the metal substrate through precipitation mechanisms (CeO_2).

Finally, an accelerated immersion corrosion test was performed. Bare AA2024 substrates and integrated self healing system A3 Ce GTL were maintained under immersion in 3.5 wt% NaCl during 75 days. NACE/ASTM TMO169/G31 test is a straightforward and simple but very visual method to follow the evolution and extension of corrosion in aggressive solutions. Fig. 10 shows the images of degradation surfaces of both samples from 1 day to 75 days (2.5 months) of immersion.

The bare AA2024 substrate shows visible signals of corrosion after 1 day of immersion that rapidly extend up to the total destruction of the alloy. In contrast, the integrated system shows no signals of degradation, color change, peeling or crack formation after 75 days of immersion in 3.5 wt% NaCl.

Thus, the proposed integrated self healing protecting system showed a very high barrier performance along with an excellent self healing ability compared with any other reported solution. Therefore, this system is proposed as a suitable alternative for producing chromium free systems for active protection of aluminum alloys.

4. Conclusions

A new integrated self healing protecting system was developed by combining an anodization process with the deposition of inhibiting sol

gel coatings (cerium glass like coating plus hybrid silica coating) on AA2024 substrates.

Homogenous, thick and porous aluminum oxide layers were prepared on AA2024 samples by anodic oxidation process using 2.5 M H_2SO_4 acid solution and applying a potential of 12 V for 30 min that corresponds with maximum thickness value of ~50 μm and pores size of 15 18 μm.

Starting from these anodizing conditions, the deposition of a silica sol gel coating allows a uniform coverage of the entire anodized surface, causing the decrease of the corrosion current density four orders of magnitude. The formation of a passivation region ($\sim 10^{-10}$ A/cm^{-2}) indicates the excellent barrier effect of the anodized sample coated with a silica sol gel coating.

The infiltration of the anodized layer and deposition of an inter medium cerium glass like coating completed by the hybrid silica barrier coating leads to an integrated self healing system. The corrosion behavior evaluated by potentiodynamic and EIS measurements revealed the excellent corrosion properties and evidenced the presence of self healing behavior in the system. The polarization resistance was not possible to measure because the current density of the integrated self healing system is higher than the detection limit of the equipment ($> 10^{-12}$ A/cm^{-2}).

EIS measurements showed a great increment of the impedance modulus at low frequency with the immersion time (from 1×10^6 Ω cm^2 to ~2.8×10^8 Ω cm^2), certifying the self healing behavior of the integrated system. These results were confirmed by an accelerated corrosion test in which the system did not show any corrosion signal after immersion in 3.5 wt% during 75 days.

The integrated hybrid silica system is a promising system, with excellent corrosion protection, including resistance to corrosion, adhesion and self healing effect, without comparison with any reported issue up to the best of our knowledge. This permits to propose this system as a useful and efficient solution for substituting CCC and CAA coatings in aircraft and aerospace sectors in the future.

CRediT authorship contribution statement

Yolanda Castro: Conceptualization, Investigation, Formal analysis, Visualization, Writing original draft, Writing review & editing, Supervision. **Eren Özmen:** Investigation, Formal analysis. **Alicia Durán:** Supervision, Formal analysis, Writing review & editing, Funding acquisition.

Acknowledgements

Declaration of competing interest

The authors declare no conflict of interest.

References

[1] S. Wernick, R. Pinner, P.G. Sheasby, The Surface Treatment and Finishing of Aluminium and Its Alloys, 5th ed., 1 Finishing Publication, Teddington, U.K, 1986.

[2] M. García-Rubio, M.P. de Lara, P. Ocón, S. Diekhoff, M. Beneke, A. Lavía, I. García, Effect of postreatment on the corrosion behaviour of tartaric–sulphuric anodic films, Electrochim. Acta 54 (2009) 4789–4800.

[3] G. Boisier, A. Lamure, N. Pébère, N. Portail, M. Villatte, Corrosion protectin of AA2024 sealed anodic layers using the hydrophobic properties of carboxylic acids, Surf. Coat. Techn. 203 (2009) 3420–3426.

[4] M. García-Rubio, P. Ocón, M. Curioni, G.E. Thompson, P. Skeldon, A. Lavía, I. García, Degradation of the corrosion resistance of anodic oxide films through immersion in the anodising electrolyte, Corros. Sci. 52 (2010) 2219–2227.

[5] G. Boisier, N. Pébère, C. Druez, M. Villatte, S. Suel, FESEM and EIS study of sealed AA2024 T3 anodized in sulfuric acid electrolytes: influence of tartaric acid, J. Electrochem. Soc. 155 (2008) C521–C529.

[6] Directive 2000/53/EC of the European Parliament and of the Council 2000, 34 and Council Decision 2005/673/EC of 20 September, 69 (2005).

[7] R.B. Figueira, C.J.R. Silva, E.V. Pereira, Organic–inorganic hybrid sol–gel coatings for metal corrosion protection: a review of recent progress, J. Coat. Technol. Res. 12 (1) (2015) 1–35.

[8] R.B. Vignesh, M.G. Sethuraman, Enhancement of corrosion protection of 3-glycidoxypropyltrimethoxysilane-based sol-gel coating through methylthiourea doping, J. Coat. Technol. Res. 1 (4) (2014) 545–554.

[9] T.T. Thai, M.-E. Druart, Y. Paint, A.T. Trinh, M.-G. Olivier, Influence of the sol-gel mesoporosity on the corrosion protection given by an epoxy primer applied on aluminium alloy 2024–T3, Prog. Org. Coat. 121 (2018) 53–63.

[10] R.B. Vignesh, T.N. Jebakumar, I. Edison, M.G. Sethuraman, Sol-gel coating with 3-mercaptopropyltrimethoxysilane as precursor for corrosion protection of aluminium metal, J. Mater. Sci. Techn. 30 (2014) 814–820.

[11] A. Durán, Y. Castro, A. Conde, J.J. Damborenea, Chapter 19, sol–gel protective coatings for metals, in: S. Sakka (Ed.), Handbook of Sol-Gel Science and Technology, Processing, Characterization and Applications, Kluwer Academic Publishers, 2005.

[12] U. Tiringer, I. Milošev, A. Durán, Y. Castro, Hybrid sol–gel coatings based on GPTMS/TEOS containing colloidal SiO$_2$ and cerium nitrate for increasing corrosion protection of aluminium alloy 7075-T6, J. Sol-Gel Sci. Techn. 85 (3) (2018) 546–557.

[13] L. Paussa, F. Andreatta, N.C. Rosero Navarro, A. Durán, L. Fedrizzi, Study of the effect of cerium nitrate on AA2024-T3 by means of electrochemical micro-cell technique, Electrochim. Acta 70 (2012) 25–33.

[14] L. Paussa, N.C. Rosero Navarro, F. Andreatta, M. Aparicio, Y. Castro, A. Durán, L. Fedrizzi, Inhibition effect of cerium nitrate solutions on the electrochemical behaviour of bare AA2024-T3, Surf. Interface Anal. 42 (2010) 299–305.

[15] E. Shchukina, H. Wang, D.G. Shchukin, Nanocontainer-based self-healing coatings: current progress and future perspectives, Chem. Commun. 55 (2019) 3859–3867.

[16] M.F. Montemor, D.V. Snihirova, M.G. Taryba, S.V. Lamaka, I.A. Kartsonakis, A.C. Balaskas, G.C. Kordas, J. Tedim, A. Kuznetsova, M.L. Zheludkevich, M.G.S. Ferreira, Evaluation of self-healing ability in protective coatings modified with combinations of layered double hydroxides and cerium molibdate nanocontainers filled with corrosion inhibitors, Electrochim. Acta 60 (2012) 31–40.

[17] M. Zheludkevich, D.G. Shchukin, K.A. Yasakau, H. Mohwald, M.G.S. Ferreira, Anticorrosion coatings with self-healing effect based on nanocontainers impregnated with corrosion inhibitor, Chem. Mater. 19 (2007) 402–411.

[18] D.G. Shchukin, M. Zheludkevich, K. Yasakau, S. Lamaka, M.G.S. Ferreira, H. Mohwald, Layer-by-layer assembled nanocontainers for self-healing corrosion protection, Adv. Mater. 18 (2006) 1672–1678.

[19] J.B. Cambon, F. Ansart, J.P. Bonino, V. Turq, Effect of cerium concentration on corrosion resistance and polymerization of hybrid sol–gel coating on martensitic stainless steel, Prog. Org. Coat. 75 (2012) 486–493.

[20] N.C. Rosero-Navarro, S.A. Pellice, A. Durán, M. Aparicio, Effects of Ce-containing sol–gel coatings reinforced with SiO$_2$ nanoparticles on the protection of AA2024, Corr. Sci. 50 (2008) 1283–1291.

[21] N.C. Rosero-Navarro, P. Figiel, R. Jedrzejewski, Y. Castro, M. Aparicio, S.A. Pellice, A. Durán, Influence of cerium concentration on the structure and properties of silica-methacrylate sol–gel coatings, J. Sol-Gel Sci. Technol. 54 (2010) 301–311.

[22] N.C. Rosero-Navarro, M. Curioni, R. Bingham, A. Duran, M. Aparicio, R.A. Cottis, G.E. Thompson, A. Durán, Electrochemical techniques for practical evaluation of corrosion inhibitor effectiveness. Performance of cerium nitrate as corrosion inhibitor for AA2024T3 alloy, Corr. Sci. 52 (10) (2010) 3356–3366.

[23] N.C Rosero-Navarro, Y. Castro, M. Aparicio, A. Duran. Recubrimientos vítreos realizados por sol–gel para la proteccion de metales frente a la corrosion, Patent: P200930982.

[24] N.C. Rosero-Navarro, M. Curioni, Y. Castro, M. Aparicio, G.E. Thompson, A. Durán, Glass-like CexOysol–gel coatings for corrosion protection of aluminium and magnesium alloys, Surf. Coat. Techn. 206 (2011) 257–264.

[25] E. Abdullayev, V. Abbasov, A. Tursunbayeva, V. Portnov, H. Ibrahimov, G. Mukhtarova, Y. Lvov, Self-healing coatings based on halloysite clay polymer composites for protection of copper alloys, ACS Appl. Mater. Interf. 5 (2013) 4464–4471.

[26] T.C. Mauldin, J.D. Rule, N.R. Sottos, S.R. White, J.S. Moore, Self-healing kinetics and the stereoisomers of dicyclopentadiene, J. R. Soc. Interface 4 (2007) 389–393.

[27] A.S. Jones, J.D. Rule, J.S. Moore, S.R. White, N.R. Sottos, Catalyst morphology and dissolution kinetics of self-healing polymers, Chem. Mater. 18 (2006) 1312–1317.

[28] K.S. Toohey, N.R. Sottos, J.A. Lewis, J.S. Moore, S.R. White, Self-healing materials with microvascular networks, Nat. Mater. 6 (2007) 581–585.

[29] Y.C. Yuan, M.Z. Rong, M.Q. Zhang, J. Chen, G.C. Yang, X.M. Li, Self-healing polymeric materials using epoxy/mercaptan as the healant, Macromolecules 4 (2008) 5197–5202.

[30] M. Oki, E. Charles, Chromate conversion coating on Al–0.2 wt.% Fe alloy, Mater. Lett. 63 (23) (2009) 1990–1991.

[31] J. Zhao, L. Xia, A. Sehgal, D. Lu, G.S. Frankel, Effects of chromate and chromate conversion coatings oncorrosion of aluminum alloy 2024-T3, Surf. Coat. Techn. 140 (1) (2001) 51–57.

[32] M. Xiangfeng, W. Guoying, G. Hongliang, Y. Yundan, C. Ying, H. Dettinger, Anodization for 2024 Al alloy from sulfuric-citric acid and anticorrosion performance of anodization films, Int. J. Electrochem. Sci. 8 (2013) 10660–10671.

[33] M. Kazemi, I. Danaee, D. Zaarei, The effect of pre-anodizing on corrosion behavior of silicate conversion coating on AA2024, Mater. Chem. Phys. 148 (2014) 223–229.

[34] V.R. Capelossi, M. Poelman, I. Recloux, R.P.B. Hernandez, H.G. de Melo, M.G. Olivier, Corrosion protection of clad 2024 aluminum alloy anodized in tartaric-sulfuric acid bath and protected with hybrid sol–gel coating, Electrochim. Acta 124 (2014) 69–79.

[35] M. Whelan, T. Edmond, J. Cassidy, J. Colreavy, B. Duffy, Optimisation of anodic oxidation of aluminium for enhanced adhesion and corrosion properties of sol-gel coatings, J. Electrochem. Soc. 163 (5) (2016) C1–C8.

[36] M. Whelan, K. Barton, J. Cassidy, J. Colreavy, B. Duffy, Corrosion inhibitors for anodised aluminium, Surf. Coat. Techn. 227 (2013) 75–83.

[37] M. Whelan, J. Cassidy, B. Duffy, Sol–gel sealing characteristics for corrosion resistance of anodised aluminium, Surf. Coat. Techn. 235 (2013) 86–96.

[38] M. Teradaa, F.M. Queiroz, D.B.S. Aguiar, V.H. Ayusso, H. Costenaro, M.G. Olivier, H.G. de Melo, I. Costa, Corrosion resistance of tartaric-sulfuric acid anodized AA2024-T3 sealed with Ce and protected with hybrid sol–gel coating, Surf. Coat. Techn. 372 (2019) 422–426.